11th International Conference on Vibration Problems
Z. Dimitrovová *et.al.* (eds.)
Lisbon, Portugal, 9–12 September 2013

EXPERIMENTAL VALIDATION OF THE ACT-AND-WAIT CONTROL CONCEPT THROUGH THE AEROPENDULUM

Giuseppe Habib*[1,2], Akos Miklos[2], Eniko T. Enikov[3], Gabor Stepan[2], Giuseppe Rega[1]

[1]Sapienza University of Rome - Dep. of Structural Engineering
{giuseppe.rega, giuseppe.habib}@uniroma1.it

[2]Budapest University of Technology and Economics - Dep. of Applied Mechanics
{miklosa, stepan}@mm.bme.hu

[3]University of Arizona - Dep. of Aerospace and Mechanical Engineering
enikov@engr.arizona.edu

Keywords: Aeropendulum, Act-and-Wait, Digital Control, Time Delay.

Abstract. *Digitization and time delay are known to modify the stability properties of feedback controlled systems. Although their effects have been widely investigated and they concern most of the systems equipped with digital processors, they are usually neglected in industrial approaches, by virtue of the high sampling frequencies of modern processors. However, these approaches are not conservative with respect to stability. Insperger and Stepan [1] introduced the act-and-wait control concept, i.e. a periodic controller that allows enlarging the stability domain of a delayed feedback controller, through a periodic variation (on-off) of the control gains. Furthermore, this controller allows obtaining faster convergence to the desired position, if not deadbeat control.*

In this work, we applied the act-and-wait controller to the so-called Aeropendulum [2], i.e. a pendulum equipped with a propeller at its end, capable of giving the required control force to the pendulum itself. The implemented controller is a simple proportional-derivative one, working in a feedback loop. The controller reads the position of the pendulum in input and sends a signal to the driving motor of the propeller in output. The system has been modeled as a 1.5 DoF system, half related to the propeller blades, modeled as a first order system, and one related to the pendulum itself. Thus, the system has dimension three: angular velocity of the propeller blades, angular position and velocity of the pendulum.

Although the system presents several nonlinearities (sinusoidal restoring force, asymmetric properties of the propeller, saturation of the control force, dry friction and quadratic damping), a linear approach allowed us to accurately estimate its stability properties. In spite of the low-cost and simplicity of the experimental setup, numerical and experimental results are in good agreement and they confirm the effectiveness of the act-and-wait controller in terms of both fast convergence and large stable region. The good matching of numerical and experimental results has been confirmed also when introducing additional delay in the control loop.

1 INTRODUCTION

Digitization and time delay are important parameters in control systems, often underestimated during stability analyses. Although several works [3, 4] show the importance of considering the digitization of the controller, the typical industrial approach consist of neglecting the finite sampling frequency by virtue of its typically high value. In force control, particular ratios between the sampling frequency and the natural frequency of the system can cause instabilities [3]. This can occur also in the case of high sampling frequencies, if the contact surface is very stiff.

The act-and-wait controller is a periodic controller, introduced for control systems with feedback delay. Its concept consists in switching on and off the controller for specific time periods, where the off period is equal or larger than the delay of the system. This concept was first introduced by Insperger and Stepan in [1, 5] for continuous time systems with feedback delay. The main idea of this controller is to wait the effects of the control force before applying it again. In particular, for continuous time control systems, feedback delays introduce infinite number of poles, making it very hard to stabilize them through an appropriate pole placement. The act-and-wait controller reduces the poles of the system to a finite number, which allows to position them more easily and, furthermore, to obtain deadbeat control [5]. When applied to digital systems [6], the controller should be on for one sampling interval and off for at least r sampling intervals, where r is the number of sampling intervals of delay the system has.

In this work we will experimentally verify the importance of taking into account the finite sampling frequency of a digital controller, applied to the so-called Aeropendulum [2]. After the identification of the parameters of the system, a proportional-differential (PD) controller for the system under study is designed. A comparison of experimental and analytical/numerical results of the stability analysis validates the adopted procedure, highlighting the non-negligible effect of the sampling frequency. Finally, we will apply the act-and-wait controller to the system under study, in order to show the improved stability properties given by this controller.

2 EXPERIMENTAL SETUP

The system under study consists of a light carbon rod, connected perpendicularly to the shaft of a low-friction potentiometer (Fig. 1). At one of its edge, the rod is rigidly connected to a small DC electric motor, driven by a 5-V pulse-width modulated (PWM) signal. The potentiometer is fixed to a plastic frame, such that the rod and the motor form a rigid planar pendulum, freely rotating around the axis of the potentiometer. The motor drives a propeller, able to give a control force to the pendulum, linearly proportional to the PWM signal within a certain range.

The system is equipped with a custom-designed circuit board, which controls the voltage supplied to the motor with a resolution of 0.05 V and reads the voltage of the potentiometer, which is proportional to the angular position of the pendulum, allowing a precise identification and setting of the sampling frequency. More detailed information about the system and in particular the circuit board can be found in [2]. The control of the system is provided by a computer interface programmed in `MATLAB` environment.

3 MODEL

The system can be modeled as a 1.5 DoF system, one related to the rigid pendulum and half related to the propeller. Regarding the propeller, it counts as half DoF since we consider only its speed of rotation (proportional to the control force) and not its angular position.

The main forces acting on the pendulum are the gravity, the dry friction in the potentiometer,

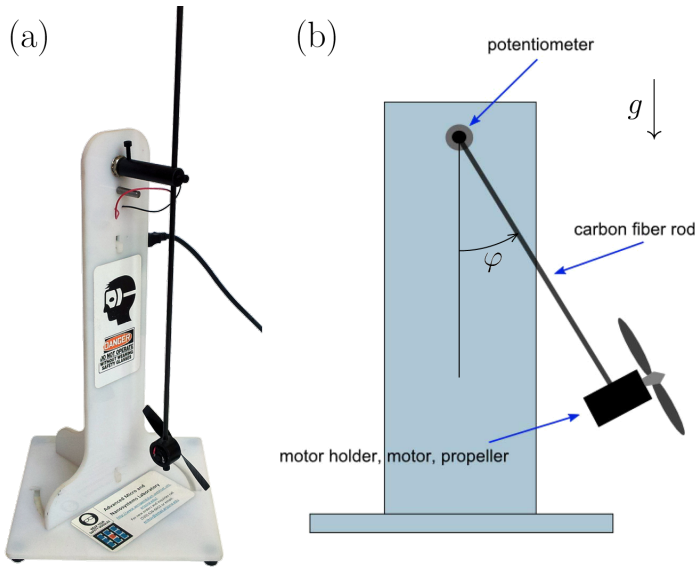

Figure 1: (a): Aeropendulum (photo); (b): schematic physical model

the air drag, the reaction force of the rod and the force given by the propeller, which depends on its speed of rotation. Neglecting the electrical dynamics of the electrical degrees of freedom, the dynamics of the propeller can be considered to be described by a first order equation. The equations of motion can be written as

$$\begin{cases} \ddot{\varphi} + 2\delta\omega_n\dot{\varphi} + \delta_2\dot{\varphi}|\dot{\varphi}| + C(\dot{\varphi})\frac{\dot{\varphi}}{|\dot{\varphi}|} + \omega_n^2\sin(\varphi) = F(\Omega) \\ \dot{\Omega} = -\frac{\Omega}{\lambda} + \frac{Q(\text{PWM})}{\lambda} \end{cases} \tag{1}$$

where φ is the angle of rotation of the pendulum, ω_n is its natural frequency, δ is the linear damping ratio, δ_2 is the coefficient of the quadratic damping (related to air drag), $C(\dot{\varphi})$ is the dimensionless dry friction, which depends on the angular velocity of the pendulum, and $F(\Omega)$ is the dimensionless force given by the propeller, which depends on the speed of rotation of the propeller. Regarding the second equation of (1), Ω represents the speed of rotation of the propeller, λ is the characteristic time of the system and the control force Q is linearly proportional to the PWM signal received in input by the motor.

Since we have no direct information about the speed of rotation of the propeller, the variable Ω is not the actual velocity of rotation of the propeller, but only a mathematical auxiliary variable. This allows us to take into account that the system has an extra half DoF, affecting the dynamics of the pendulum, without need of calculating the exact value of the speed of rotation.

4 ESTIMATION OF THE COEFFICIENTS

The system under study is rather simple, however, we have no specifications about the geometry and material properties of the single components. Thus, it is necessary to perform experiments in order to define the coefficients of Eq. (1) and the functions $C(\dot{\varphi})$ and $F(\Omega)$.

4.1 Pendulum coefficients

First, we let the pendulum oscillate with free vibrations. This allows us to eliminate the variable Ω and the force F, letting the simpler system

$$\ddot{\varphi} + 2\delta\omega_n\dot{\varphi} + \delta_2\dot{\varphi}|\dot{\varphi}| + C(\dot{\varphi})\frac{\dot{\varphi}}{|\dot{\varphi}|} + \omega_n^2\sin(\varphi) = 0 \tag{2}$$

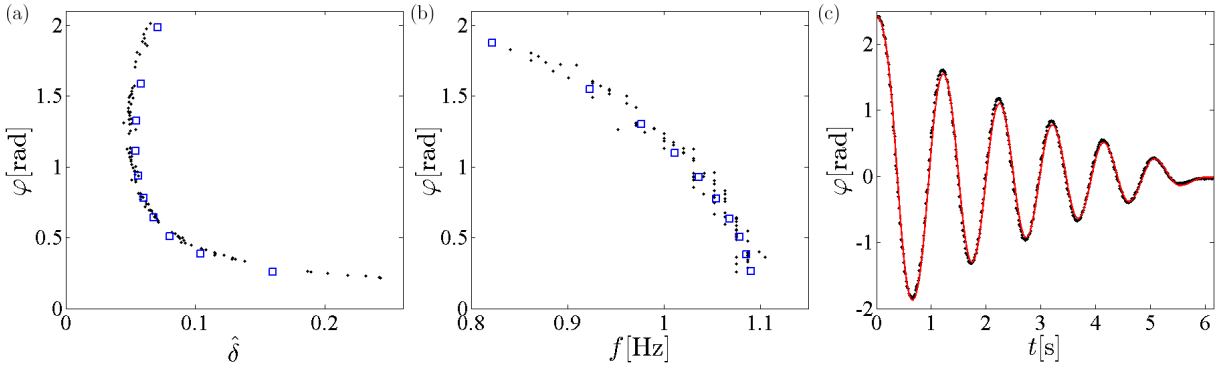

Figure 2: Experimental (black dots) and numerical (blue squares) damping backbone (a) and frequency backbone (b) curves. The experimental results are obtained from a superposition of ten different free vibration decays. (c): free vibration decay; black dots: experimental result, solid red line: numerical result. For the numerical simulations: $\omega_n = 6.9$ rad/s, $\delta = 0$, $\delta_2 = 0.028$ rad^{-1}, $\beta = 2$, $\mu_0 = 2.6$ rad/s^2 and $\alpha = 0.77$ ($\mu_0(1+\alpha) = 4.6$ rad/s^2).

The dry friction has been modeled with the exponential function $C_{\max}(\dot{\varphi}) = \mu_0 \left(1 + \alpha e^{-\beta|\dot{\varphi}|}\right)$. The value of $\mu_0(1+\alpha)$ can be directly estimated slowly moving the pendulum from the zero position and verifying which is the maximal angle different from zero that still gives an equilibrium position. This approach gave the estimation $\mu_0(1+\alpha) \approx (0.0949 \pm 0.01)\,\omega_n^2$. Variations depend on air temperature and humidity.

Since the system is subject to softening, it is not trivial to estimate the value of ω_n. Similarly, all other coefficients cannot be directly estimated from the free vibration decay. In order to find them, we plotted several experimental free vibration decays and for all of them we plotted the damping and the frequency backbone curves (in Fig. 2 the superposition of several free vibration decays).

The frequency backbone curve has been obtained calculating the instantaneous periods, i.e. the distance between two subsequent peaks, and then calculating the frequency as its inverse. The curve clearly shows the expected softening behavior. Furthermore, it seems to converge to the value $f = 1.1$ Hz, which should be the value of the linear natural frequency.

The damping backbone curve has been obtained calculating, for each couple of subsequent peaks, the logarithmic decrement. Then, from the logarithmic decrement, the equivalent linear damping is calculated according to the formula $\hat{\delta} = 1/\sqrt{1 + (2\pi/d)}$, where d is the logarithmic decrement. Although different from other definitions of damping backbone given in the literature [7, 8], this procedure gives an estimate of the linear damping that would be necessary to obtain an equivalent decrement, given by all the damping components (so not only the linear one), as a function of the amplitude. Considering that the damping is mainly given by dry friction and (quadratic) air drag, the result shown in Fig. 2(a) is not surprising. The quadratic damping is dominant over the linear one for large amplitudes, while the dry friction is dominant over the linear damping for small amplitudes of oscillation. Accordingly, the diagram in the figure shows that for small amplitude a very large linear damping would be required to have the same effect of the dry friction. The value of $\hat{\delta}$ reduces increasing the amplitude of oscillation, until the curve bends forward again due to the increasing relevance of the air drag.

A comparison of the damping and frequency backbone curves and of the free vibration decay obtained by several experiments with those obtained by numerical simulations, allows us to find an optimal set of parameter values. The chosen set of parameters is $\omega_n = 6.9$ rad/s, $\delta = 0$ (no linear damping), $\delta_2 = 0.028$ rad^{-1}, $\beta = 2$, $\mu_0 = 2.6$ rad/s^2 and $\alpha = 0.77$. A comparison of the free vibration decays obtained experimentally and numerically with these values is given in Fig.

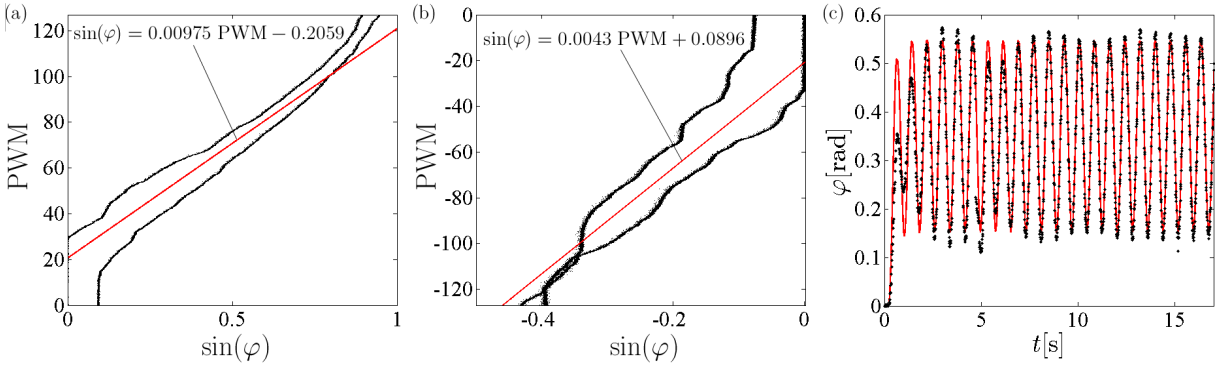

Figure 3: PWM vs. $\sin(\varphi)$ signal for increasing and decreasing values of PWM. Straight red line: linear interpolation of mean values in the linear range. (a): positive values of PWM; (b): negative values of PWM. (c): Experimental (black dots) and numerical (red solid line) force vibration response for PWM $= 60 + 30\sin(8t)$. For the numerical simulation: $\lambda = 0.28$ s, $\omega_n = 6.9$ rad/s, $\delta = 0$, $\delta_2 = 0.028$ rad^{-1}, $\beta = 2$, $\mu_0 = 2.6$ rad/s^2 and $\mu_0(1+\alpha) = 4.6$ rad/s^2.

2(c) (red line numerical result), while the blue squares in Figs. 2(a) and (b) show the numerical backbone curves.

4.2 Propeller force

The PWM signal can be considered linearly proportional to Q and it can be easily verified that for constant values of Q, Ω will tend asymptotically to Q. Giving slowly varying input signals to the motor, it is possible to define the function $F(\text{PWM})$. Neglecting for the moment the dry friction, the equilibrium position is given by $\omega_n^2 \sin(\varphi) = F(\Omega) = F(Q(\text{PWM}))$, of course, due to the dry friction, the system has infinitely many equilibrium positions around this one.

PWM signal values, acceptable by the circuit board, must be included between -127 and +127. In order to define $F(\text{PWM})$, we first gave a slowly increasing PWM signal, from 0 to +127, to the system. Then, we repeated the procedure for slowly decreasing values of PWM, from +127 to 0, imposing an initial large displacement. After that we repeated the procedure for negative values of PWM. The result is shown in Figs. 3(a) and (b). An ideal system without friction and with a linear relation between F and PWM, should give a straight line in the PWM, $\sin(\varphi)$ space.

Fig. 3 clearly shows that increasing and decreasing values of PWM give different results, this can be attributed to the dry friction. Furthermore, it appears that for large values of PWM the force saturates. Then, a dead-band can be recognized: for $|\text{PWM}| < 20.5$ the pendulum does not move (and neither the propeller). Finally, a comparison between Figs. 3(a) and (b) shows that the force provided by the propeller is strongly asymmetric. The force provided for negative values of PWM is almost the half than the one estimated for positive values of PWM. In spite of all nonlinearities, the curves still show a linear range for $30 < |\text{PWM}| < 90$.

4.3 Propeller time constant

In order to find λ, we consider the second equation of (1) in the case of a time varying input signal. If Q is harmonic, i.e. $Q(t) = Q_0 \sin(\omega t)$, we have the differential equation $\mathrm{d}\Omega/\mathrm{d}t = -\Omega/\lambda + Q_0 \sin(\omega t)/\lambda$, that, after the transient fades away, has solution

$$\Omega(t) = \frac{Q_0}{\sqrt{1+\lambda^2\omega^2}} \sin(\omega t + \phi), \tag{3}$$

where the phase shift ϕ can be neglected for our purposes.

Now, considering the full system, in the case of a harmonic excitation through the control force Q with amplitude Q_0, due to λ the pendulum will be excited with an amplitude reduced by the factor $1/\sqrt{1+\lambda^2\omega^2}$. Since all the other parameters of the system have been already estimated, including the function $F(Q(\text{PWM}))$, a comparison of numerical and experimental results of the forced system allows us to estimate the value of λ. To simplify the simulation and improve the accuracy of the result, we add a constant value to the motor input signal, in order to avoid the dead-band and stay in the linear range of F.

Figure 3(c) shows the result of the calibration for $\text{PWM} = 60 + 30\sin(8t)$ with $\lambda = 0.28$ s. The red line is the numerical result while the black dots are the experimental one. The matching, once the system is at regime, is excellent. Furthermore, the numerical result is very sensitive to variation of λ, which gives more reliability to the estimation.

5 DESIGN OF THE CONTROLLER

We consider the stabilization of a general position φ_0 of the pendulum. In order to make that position being of equilibrium, it is necessary that the propeller gives a corresponding constant force, according to the diagram in Fig. 3. For example, giving a constant PWM signal of 80, the pendulum will stabilize around $\varphi = 0.61$ ($\sin(\varphi) = 0.00975\text{PWM} - 0.2059$). Because of the dry friction and uncertainties of the estimated coefficients, the pendulum will stabilize in a position close to the desired one, but not exactly there. An active control can improve both the correct positioning and the speed of convergence to the desired position.

The controller implemented in the system is a classical PD controller, defined as $F = -k_P(\varphi - \varphi_0) - k_D\dot{\varphi}$, where F is the control force and k_P and k_D are respectively the proportional and the differential gain. In the system under study, the control scheme needs some corrections, since it does not give a direct force to the pendulum, but it can only send modulated PWM signals to the motor driving the propeller.

First of all, it is necessary to compensate the dead-band, thus, we should add 20.5 (-20.5) to the PWM signal if it is positive (negative). Besides the dead-band, $F(\text{PWM})$ is linear with a good approximation, until saturation occurs for $|\text{PWM}| > 90$. Then, we should consider the slope of the curve in Fig. 3, in order to associate a value of PWM to a force. For positive values of PWM, besides the dead-band, we have that the force provided by the propeller is $F = 0.00975\omega_n^2\text{PWM}$ rad/s^2, while for negative values of PWM $F = 0.0043\omega_n^2\text{PWM}$ rad/s^2, within the linear range.

Furthermore, we should consider that the controller works at discrete time intervals. Thus, it samples the PWM signal at the time instants $t_j = j\tau$, $j = 0, 1, 2, ...$, where τ stands for the sampling time and $f_s = 1/\tau$ is the sampling frequency. PWM is then piecewise constant in the sampling interval and it is calculated from the position sampled at the beginning of the previous sampling interval. Moreover, the velocity should be calculated numerically. Calling $\varphi_j = \varphi(t_j)$ and $\text{PWM}_j = \text{PWM}(t_j)$, we can define the control scheme as

$$\begin{aligned}\text{PWM}_{j+1} &= -k_P\left(\varphi_j - \varphi_0\right) - k_D\frac{\varphi_j - \varphi_{j-1}}{\tau} + \text{PWM}_0 \\ &\quad +20.5 \times \text{sign}\left(-k_P\left(\varphi_j - \varphi_0\right) - k_D\frac{\varphi_j - \varphi_{j-1}}{\tau} + \text{PWM}_0\right), \end{aligned} \tag{4}$$

where $\text{PWM}_0 = \sin(\varphi_0)/a$ is related to the constant part of the control force. This gives the

following system of equations

$$\begin{cases} \ddot{\varphi} + \delta_2 \dot{\varphi}|\dot{\varphi}| + C(\dot{\varphi})\frac{\dot{\varphi}}{|\dot{\varphi}|} + \omega_n^2 \sin(\varphi) = a\omega_n^2 \Omega \\ \dot{\Omega} = -\frac{\Omega}{\lambda} + \frac{\text{PWM}_j}{\lambda} \\ a = \begin{cases} 0.00975 \text{ s/rad} & \text{if} \quad \Omega > 0 \\ 0.0043 \text{ s/rad} & \text{if} \quad \Omega < 0 \end{cases} \end{cases} \qquad t \in [t_j, t_{j+1}) \tag{5}$$

with PWM given by Eq. (4). As already mentioned, in this formulation Ω has no physical meaning, but it is still expressed in rad/s. It should also be noted that the circuit board of the pendulum allows only integer PWM signals in input. This mathematical model could be improved considering the saturation of the propeller force, easily obtainable from Fig. 3.

6 ESTIMATION OF STABILITY

As already mentioned, because of the non-negligible dry friction, given a constant PWM input signal, the pendulum has a full range of equilibrium positions. Considering the system in Eq. (5) in steady state conditions, where φ_0 is the desired position and PWM_0 is the signal calculated to make φ_0 being of equilibrium, we have

$$C(\dot{\varphi}) + \omega_n^2 \sin(\varphi) = a\omega_n^2 \left(\text{PWM}_0 - k_P \left(\varphi - \varphi_0\right)\right), \tag{6}$$

where $a\text{PWM}_0 = \sin(\varphi_0)$. In the case of no active control ($k_P = 0$) the maximal positioning error is $\epsilon \approx |\mu_0(1+\alpha)/\left(\omega_n^2 \cos(\varphi_0)\right)|$. While, the proportional control gain reduces the maximal positioning error according to the formula $\epsilon_P \approx |\mu_0(1+\alpha)/\left[\omega_n^2 \left(\cos(\varphi_0) + ak_P\right)\right]|$, thus, it is clear that high proportional gains sensibly improve the positioning of the system. On the other side, too large values of k_P could destabilize the system, as well.

The estimation of stability of an equilibrium position of a system with the dry friction is controversial. Considering the equilibrium position φ_0, there will always exist a φ_e, with $|\varphi_e - \varphi_0|$ arbitrarily small, such that φ_e is also an equilibrium position. Thus, it can be proven that the system, as expressed in Eq. (5), is always stable (but never asymptotically stable) in the sense of Lyapunov.

Terms of order lower than the first, as in the case of a system with dry friction, make the traditional linear stability analysis meaningless, thus it is necessary to use another approach to have a significant engineering parameter. Our approach consists in substituting the dry friction with a linear damping, which has an equivalent effect for certain amplitudes of oscillation (see Fig. 2(a)). The value chosen for the following investigation is $\hat{\delta} = 0.065$. A stability analysis of such a linearized system should estimate if the real system is converging or not to the desired position, while it oscillates around it with a certain amplitude. Of course the nonlinear behavior of the real system is much more complex than that and it may have a complicated basin of attraction, still this approach may provide a significant approximation.

Linearizing $\sin(\varphi)$ as well around a general position φ_0, we obtain the equation

$$\begin{cases} \ddot{\varphi} + 2\hat{\delta}\omega_n \dot{\varphi} + \omega_n^2 \left(\sin(\varphi_0) + \cos(\varphi_0)(\varphi - \varphi_0)\right) = a\omega_n^2 \Omega \\ \dot{\Omega} = -\frac{\Omega}{\lambda} + \frac{\text{PWM}_j}{\lambda} \\ \text{PWM}_{j+1} = -k_P \left(\varphi_j - \varphi_0\right) - k_D \frac{\varphi_j - \varphi_{j-1}}{\tau} + \text{PWM}_0 + 20.5 \end{cases} \qquad t \in [t_j, t_{j+1}) \tag{7}$$

where $a = 0.00975$ and $\text{PWM}_0 = \sin(\varphi_0)/a$. The linear asymmetry of the controller is eliminated if φ_0 is chosen such that the control force is always positive or always negative around φ_0, which simplifies the stability analysis of the system.

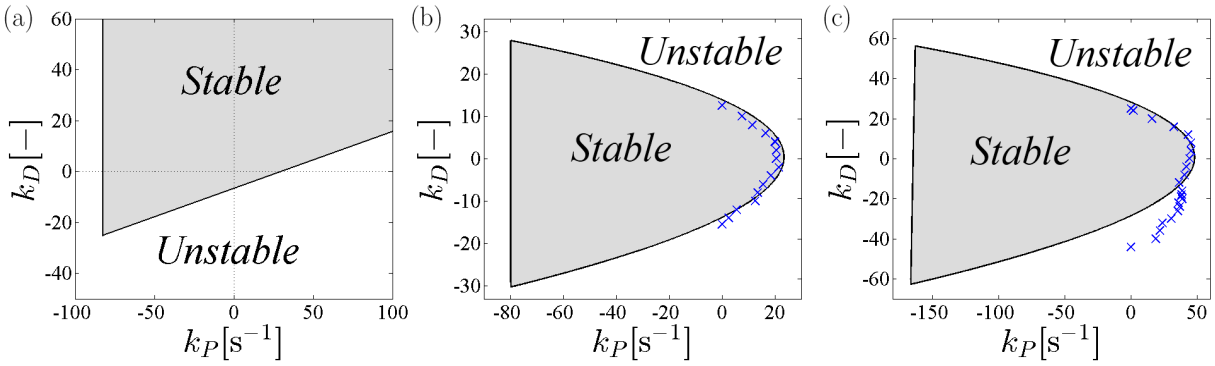

Figure 4: Stability chart of the system in Eq. (7) around the point $\varphi_0 = 0.64$ rad. (a): continuous time approach (or $\tau \to 0$); (b): discrete time, $\tau = 0.05$, $r = 1$; (c): act-and-wait controller, $\tau = 0.05$, $r = 1$. Blue $\times$-s refer to the experimental border of stability.

The system in Eq. (7) is piecewise linear and can be analyzed by solving it in closed form for each time step and reducing it to a map. This lengthy operation can be easily performed with computer algebra. The resulting formulas are however not interesting in this context, thus are omitted here and only some significant stability charts are presented. For analogous calculations see [4].

6.1 Stability charts and other results

Fig. 4(b) shows the stability chart in the k_P, k_D space obtained for $\tau = 0.05$ s around the position $\varphi_0 = 0.64$. The system admits stable solutions in a large area of negative values of k_P. This is due to the restoring force that compensate negative values of the proportional control gain. However, the whole region with $k_P < 0$ is not of practical interest, since in that case the control force is worsening the accuracy of the positioning. Negative values of k_D are instead acceptable since derivative control has only dynamical effects.

The blue $\times$-s in the figure indicate the border of the experimental stability chart, for positive values of k_P. As we already mentioned, the real system is strongly nonlinear and solutions depend on their initial conditions. Thus, in order to have a significant result, the trial to verify the stability of the system for each pair of control gains was performed using approximately the same initial conditions $\varphi = 0$ and $\dot{\varphi} = 0$.

In spite of the numerous simplifications performed to linearize the system, the matching between the analytical/numerical and experimental results is satisfactory, both from a qualitative and from a quantitative point of view. The good matching confirms the practical significance of the investigated stability.

Fig. 4(a) shows the stability chart obtained in the theoretical case of a continuous time approach, which corresponds to the digital system where $\tau \to 0$. The stability chart is unbounded and it can be obtained analytically.

It should be noted that the minimal allowed value of k_P in order to have stability is the same in the continuous and in the discrete time approach. This occurs because values of k_P below the stability boundary make a statical loss of stability occur, and not a dynamical one, as when crossing any other stability boundary. Furthermore, this border is independent of the value of λ. On the other hand, the stability chart for positive values of k_P is totally different in the two cases. The good agreement between the numerical and the experimental results highlights the importance of considering the digitization of the controller.

Fig. 4(c) shows an analogous stability chart in the case of the application of the act-and-wait

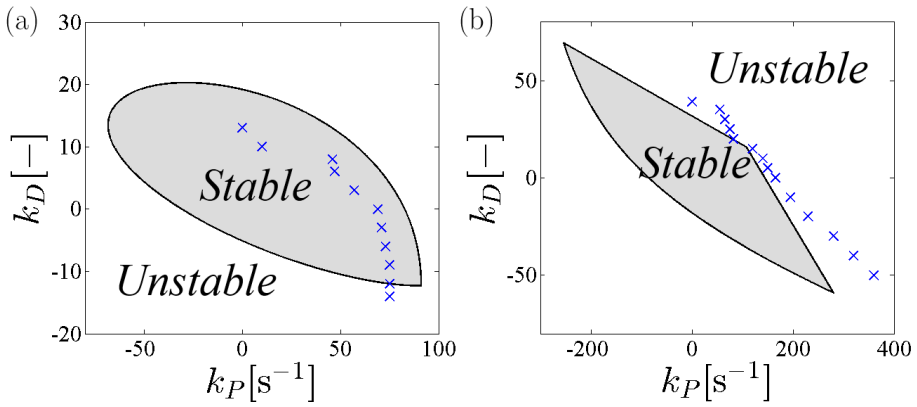

Figure 5: Stability chart of the system in Eq. (7) around the point $\varphi_0 = 0.64$ rad. (a): normal controller; (b): act-and-wait controller. $\tau = 0.3$ s, $r = 2$. Blue $\times$-s refer to the experimental right border of stability.

controller. A comparison of Figs. 4(b) and (c), shows that the stability chart in the case of the act-and-wait controller is almost exactly the double than in the case of a normal PD controller. This result is expected considering that the inertia of the propeller acts as a low-pass filter (see Eq. (3)), almost halving the effective gain of the controller for low values of τ. In order to verify the actual effectiveness of the act-and-wait controller it is necessary to increase the sampling time of the system.

Fig. 5 shows the stability chart in the case of a delayed system, where the controller acts according to the position and velocity sampled r time intervals before the actuation. In the figure $r = 2$. In this case, the act-and-wait controller acts only for one third of the time. Since the sampling time has been sensibly increased ($\tau = 0.3$ s), the effect of the act-and-wait controller is not anymore filtered out by the propeller inertia.

The blue-$\times$ in Fig. 5 mark the right stability border defined experimentally. The matching is not as good as the one of Fig. 4, but it is still acceptable, considering the large simplification adopted. The mismatch is probably due to the more involved basin of attraction of the desired solution. A comparison of Figs. 5(a) and (b) clearly shows the enlarged stability chart in the case of the act-and-wait controller.

Fig. 6(a) shows the positioning error, with respect to the desired position, obtained with different values of the control gain. Experimental results clearly show the improvement obtained with higher control gains. The mismatch with the analytical result is partially due to the fact that, if the position of the pendulum is different from zero, the dry friction reduces because of the decreased load on the hinge. In addition, the vibrations given by the propeller help the pendulum moving towards the equilibrium position in spite of the dry friction.

Considering the linearized system in Eq. (7), it is possible to estimate the vibration frequency of the system at the loss of stability, which is given by $f = \alpha / (2\pi\tau)$, where α is the arctangent of the ratio between the imaginary and the real part of the characteristic multiplier related to the loss of stability. For the case of a normal controller, with $\tau = 0.05$ s and $\varphi_0 = 0.64$, the result is shown in Fig. 6(c). The matching between the experimental results (blue squares) and the analytical ones (dashed line) is satisfactory.

7 CONCLUSIONS

In this work, we investigated the stability of a digital PD controller applied to the so-called Aeropendulum. After an identification of the parameters of the model, the effectiveness of a linearized procedure aimed at investigating the practical stability of a system subject to dry fric-

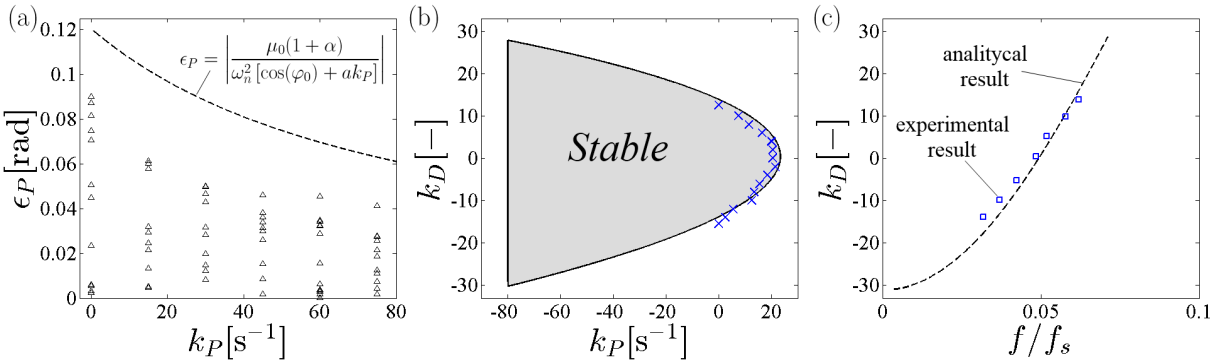

Figure 6: (a): Error in the positioning of the pendulum. △ experimental results; dashed line: analytical result ($\mu_0(1+\alpha) = 4.6$ rad/s^2). (b): stability chart for $\tau = 0.05$ s, $r = 1$ and $\varphi_0 = 0.64$ rad (as in Fig. 4(b)). (c): frequency of oscillation at the loss of stability; dashed line: analytical result, blue squares: experimental results.

tion has been shown. Most of the obtained experimental results are in good agreement with the analytical/numerical ones, this reinforces the reliability of the procedure and shows the importance of considering the digitization of the controller. The obtained experimental results also show the improved stability properties of the system, if the act-and-wait controller is used.

ACKNOWLEDGMENT

This research was also supported by the Hungarian National Science Foundation under grant no. OTKA 101714.

REFERENCES

[1] T. Insperger, G. Stepan, *Semi-discretization for time-delay systems – Stability and Engineering applications*, Springer, 2011.

[2] E.T. Enikov, G. Campa, Mechatronic Aeropendulum: Demonstration of linear and nonlinear feedback control principles with MATLAB/Simulink Real-Time Windows Target, *IEEE Transactions on Education*, **55**(4), 538–545, 2012.

[3] L.L. Kovacs, J. Kovecses, G. Stepan, Analysis of Effects of Differential Gain on Dynamic Stability of Digital Force Control. *Int. J. Nonlin. Mech.* **43**, 514–520, 2008.

[4] Habib, G., Rega, G., Stepan, G., Stability analysis of a two-DoF system subject to proportional-derivative digital position control. To appear in *J. Vib. and Control*

[5] T. Insperger, Concept for continuous-time control systems with feedback delay. *IET Control Sys. Tech.* **14**(5), 974–977, 2006.

[6] T. Insperger, G. Stepan, Act-and-wait control concept for discrete-time systems with feedback delay. *IET Control Theory Appl.* **1**(3), 553–557, 2007.

[7] J.B. Roberts, Estimation of nonlinear ship roll damping from free decay data. *J. of Ship Research* **29**, 127–138, 1985.

[8] O. Gottlieb, M. Feldman, Application of a Hilbert transform-based algorithm for parameter estimation of a nonlinear ocean system roll model. *J. of Offshore Mechanics and Arctic Engineering*. **119**, 239–243, 1997.